

# Growth of $\text{Pb}((\text{Zn}_{1/3}\text{Nb}_{2/3})_{0.91}\text{Ti}_{0.09})\text{O}_3$ Single Crystals Using an Allomeric Seed Crystal and Their Electrical Properties

Bijun Fang,<sup>†,‡</sup> Haiqing Xu,<sup>†</sup> Tianhou He,<sup>†</sup> Haosu Luo,<sup>†,§</sup> and Zhiwen Yin<sup>†</sup>

The State Key Laboratory of High Performance Ceramics and Superfine Microstructure, Shanghai Institute of Ceramics, Chinese Academy of Sciences, Shanghai 201800, People's Republic of China

EPCOS (Zhuhai FTZ) Co., Ltd., Hongwan, Wanzai, Zhuhai Free Trade Zone, Zhuhai City, Guangdong Province 519030, People's Republic of China

Single crystals of  $\text{Pb}((\text{Zn}_{1/3}\text{Nb}_{2/3})_{0.91}\text{Ti}_{0.09})\text{O}_3$  (PZNT 91/9), 28 mm in diameter and 30 mm in length, have been successfully grown using a modified Bridgman technique with an allomeric seed crystal. X-ray fluorescence analysis (XRFA) measurement confirms that the effect of segregation is not serious. The segregation coefficient  $k$  for  $\text{PbTiO}_3$  content during crystal growth is 0.99, which causes some fluctuation in the composition along the growth direction. The fluctuation of composition and the complicated domain structure cause a variation of electric properties. Dielectric measurement indicates that PZNT 91/9 crystals exhibit an almost normal ferroelectric phase transition at  $\sim 183^\circ\text{C}$  from the tetragonal phase to the cubic phase. In addition, a weak frequency-dependent ferroelectric–ferroelectric phase transition is observed at  $\sim 85^\circ\text{C}$ , which is attributed to partial conversion of the rhombohedral phase to a tetragonal phase. The dielectric thermal hysteresis behavior and the existence of polarization above the Curie temperature verify that the phase transitions at  $\sim 85^\circ\text{C}$  and  $183^\circ\text{C}$  are first order with a slight diffuse character and first order, respectively. It is demonstrated that the effects of segregation can be decreased and the homogeneity of the obtained PZNT 91/9 single crystals can be improved by optimizing growth parameters.

## I. Introduction

PIEZOELECTRIC crystals of solid solutions between the relaxor ferroelectric (FE) lead zinc niobate,  $\text{Pb}(\text{Zn}_{1/3}\text{Nb}_{2/3})\text{O}_3$  (PZN), and the normal ferroelectric lead titanate,  $\text{PbTiO}_3$  (PT), are better than conventional  $\text{PbZrO}_3$ – $\text{PbTiO}_3$  (PZT) because  $(1-x)\text{PZN}$ – $x\text{PT}$  (PZNT) single crystals are relatively easily grown using a flux method over a wide solid-solution range of  $0 \leq x \leq 0.2$ .<sup>1,2</sup> Substitution of  $\text{Ti}^{4+}$  ions for the complex  $(\text{Zn}_{1/3}\text{Nb}_{2/3})^{4+}$  ions on the B site results in the formation of long-range, ordered ferroelectrics. Therefore, the solid solutions of  $(1-x)\text{PZN}$ – $x\text{PT}$  are expected to combine the advantages of relaxor ferroelectric PZN and ferroelectric PT.<sup>3</sup> The morphotropic phase boundary (MPB) for the  $(1-x)\text{PZN}$ – $x\text{PT}$  system is located at  $x = 0.08$ – $0.105$ , which separates a rhombohedral phase from a tetragonal phase. Of all the solid solutions,  $\text{Pb}((\text{Zn}_{1/3}\text{Nb}_{2/3})_{0.91}\text{Ti}_{0.09})\text{O}_3$  (PZNT 91/9) with a composition near the MPB is of great interest because of its

large piezoelectric and dielectric constants. Kuwata *et al.*<sup>2</sup> have reported that (001) crystals of PZNT 91/9 exhibit an exceptionally large piezoelectric constant ( $d_{33} > 1500$  pC/N) and electromechanical coupling factor in the longitudinal bar mode ( $k_{33} > 92\%$ ). Such excellent performance makes the piezocrystals a promising candidate for next-generation electromechanical transducer materials.

From the viewpoint of crystal chemistry, the outstanding properties of the relaxor-based piezocrystals are closely related to the MPB effects and the formation of macrodomain states that result from the substitution of  $\text{Ti}^{4+}$  ions for the complex  $(\text{Zn}_{1/3}\text{Nb}_{2/3})^{4+}$  ions on the B site of the perovskite structure.<sup>3</sup> Kobayashi *et al.*<sup>4</sup> have reported large PZNT 91/9 single crystals (the largest obtained single crystal was 43 mm  $\times$  42 mm  $\times$  40 mm) grown using a conventional flux method. However, it is difficult to grow large PZNT crystals using the flux method because of its poor reproducibility and spontaneous nucleation during crystal growth. In contrast, Bridgman growth allows the fabrication of crystals with controlled dimensions and good reproducibility. Yamashita and co-workers<sup>5,6</sup> have confirmed that the Bridgman method is suitable for mass production of large PZNT 91/9 crystals for practical applications. However, to our knowledge, the growth process of PZNT 91/9 single crystals via the Bridgman method has not been studied in detail. The segregation during PZNT crystal growth is not understood in detail, and limited attention has been paid to phase transitions. To obtain large, high-quality, single crystals, we have developed a modified Bridgman technique to grow PZNT crystals using an allomeric seed crystal. The seed is of the same perovskite structure, but with a different composition. In this article, we report on the growth of PZNT 91/9 single crystals and characterize their properties.

## II Experimental Procedures

PZNT 91/9 single crystals were grown using a modified Bridgman method. The schematic diagram of the modified Bridgman furnace for the growth of PZNT 91/9 single crystals is illustrated in Fig. 1 of Ref. 7. High-purity ( $>99.9\%$ ) reagent powders of  $\text{PbO}$ ,  $\text{ZnO}$ ,  $\text{Nb}_2\text{O}_5$ , and  $\text{TiO}_2$  were dried and then weighed. The mixture of these powders was maintained in the mole percentage ratios of PZN:PT = 91:9 and PZN-PT:PbO = 45:55.  $\text{PbO}$  acted as the flux. The raw materials were precalcined using a B-site precursor synthesis method that assisted in the prevention of pyrochlore phase formation during crystal growth.<sup>8,9</sup>  $\text{ZnO}$ ,  $\text{Nb}_2\text{O}_5$ , and  $\text{TiO}_2$  powders were precalcined at  $950^\circ\text{C}$  for 1.5 h after they were mixed and mortared in V-type mixing equipment for 4–8 h. Stoichiometric  $\text{PbO}$  was added, and the powders were mixed in the same V-type mixing equipment and then postcalcined at  $750^\circ\text{C}$  for 1.5 h. The resultant powder with the addition of  $\text{PbO}$  flux was mixed using the ball-mill technique with  $\text{ZrO}_2$  balls and water for 24 h. Pellets 28 mm in diameter and 60 mm in length were obtained using the isostatic-pressing method.

S. Trolrier-McKinstry—contributing editor

Manuscript No. 187368. Received October 26, 2001; approved December 4, 2003. Supported by the National Sciences Foundation of China, under Grant Nos. 59995520 and 59872048, and by the Shanghai Municipal Government under Grant No. 005207015.

<sup>†</sup>The State Key Laboratory of High Performance Ceramics and Superfine Microstructure.

<sup>‡</sup>EPCOS.

<sup>§</sup>Author to whom correspondence should be addressed.

PZNT single crystals were fabricated in sealed platinum crucibles to prevent the evaporation of PbO during crystal growth.

During crystal growth, we introduced an allomeric  $\text{Pb}((\text{Mg}_{1/3}\text{-Nb}_{2/3})_{0.69}\text{Ti}_{0.31})\text{O}_3$  (PMNT 69/31) seed crystal rested along the  $\langle 111 \rangle_{\text{cub}}$  direction, which could effectively prevent spontaneous nucleation because of the slight structural differences between the PMNT and PZNT crystal lattices. PZNT crystals were grown at a temperature of 1250°C.<sup>6</sup> The temperature of the Bridgman furnace was regulated using a proportional integral differential (PID) controller. After the charged crucibles were soaked for 6 h in the center of the furnace, they were lowered at the rate of 0.2–0.6 mm/h. To prevent proto-cracking of the crystals during cooling, all crucibles were annealed at 700°C for 4 h. Annealing at this temperature effectively inhibited the appearance of cracking caused by thermal stress during fast cooling and without additional pyrochlore-phase formation. The furnace then was cooled to room temperature at a rate of 50°–80°C/h.

The lattice structure of the obtained PZNT crystals was investigated using powder X-ray diffractometry (XRD; Model D/MAX-3C, Rigaku Co., Tokyo, Japan). Thermogravimetric analysis (TG) and differential thermal analysis (DTA) were performed using a simultaneous micro-DTA/TG apparatus (Model STA429, Netzsch, Bayern, Germany). Samples (as-grown crystal powder and precalcined mixture powder) of ~50 mg each were heated from room temperature to ~1300°C at 10°C/min in an air atmosphere and then cooled to room temperature. The variation of composition was measured directly using X-ray fluorescence analysis (XRFA; Model PW2404, Phillips, Eindhoven, The Netherlands) with plates cut from various regions of a PZNT boule. The ferroelectric hysteresis loops of the (001) PZNT 91/9 crystal plates were tested using a standard ferroelectric test system (Model RT-66A, Radiant Technology, Inc., Fullerton, CA) with a high-voltage direct-current amplifier (Model 609C-6, Trek, Inc., Medina, NY). The strain of the samples was measured with the application of an applied electric field. The domain configuration of the obtained PZNT crystal was observed using polarized-light microscopy (Olympus Optical Co., Tokyo, Japan). The samples were cut perpendicular to the  $\langle 001 \rangle_{\text{cub}}$  direction and were finely polished.

### III. Results and Discussion

#### (1) Thermal Stability and X-ray Diffractometry Analysis

Figure 1 shows the TG and DTA analyses during heating and cooling for the precalcined powder and the ground PZNT 91/9

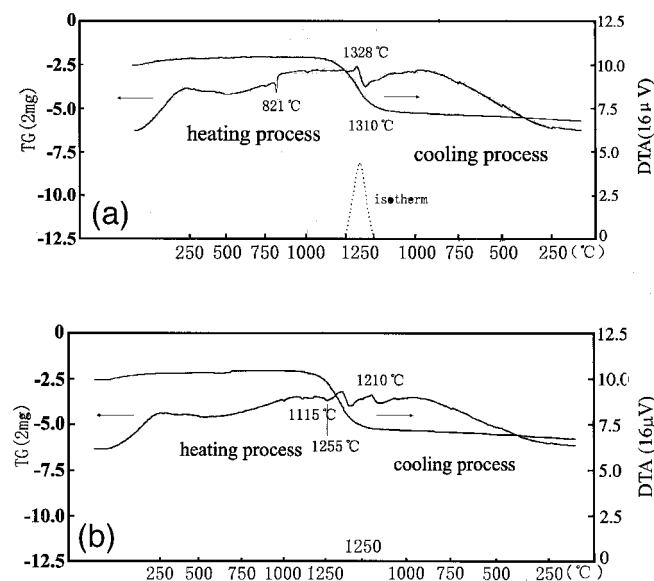


Fig. 1. DTA and TG curves during heating and cooling process for (a) precalcined mixture powder and (b) PZNT 91/9 crystal powder.

crystal powder. Figure 1(a) shows that PbO melted at 821°C. The rapid weight loss in the pretreated material started at temperatures >1180°C. A strong endothermic DTA peak was detected at 1255°C for the PZNT 91/9 crystal. In addition, a minor heat flow appeared at 1115°C, which indicated the decomposition of perovskite phase to pyrochlore phase. Serious weight loss from the PZNT crystal appeared at >1200°C, which was caused by progressive decomposition of the crystal. Hereafter, PZNT single crystals needed to be grown in sealed platinum crucibles to suppress the volatilization of PbO.

The structure of various regions of a grown PZNT 91/9 crystal was investigated using XRD with a 15 mm long crystal boule. There were no apparent differences in the XRD patterns of the initial and final parts, except for a slight splitting of the (200) diffraction peak of the final part. The splitting of the diffraction peaks was far less obvious than that of  $\text{Pb}((\text{Mg}_{1/3}\text{Nb}_{2/3})_{0.67}\text{Ti}_{0.33})\text{O}_3$  (PMNT 67/33) grown from the melt,<sup>7</sup> where the splitting of the (100), (200), (210), and (211) diffraction peaks of the final part was obvious. The decrease in splitting of various diffraction peaks suggested that the segregation during the growth of PZNT crystals was less serious than that of PMNT crystals. The splitting of the (200) diffraction peak indicated a structural phase transition from the rhombohedral phase to the tetragonal phase along the growth direction because of segregation. The appearance of tetragonal phase implied increased  $\text{PbTiO}_3$  content along the growth direction.

#### (2) Segregation during the Growth of PZNT 91/9 Single Crystals

The resulting PZNT crystal boules exhibited a dark-brown color on their surface because of a thin coat of PbO flux. After the flux was removed by boiling the crystal in acetic acid, the boules showed three appearing faces, which deviated slightly in angle from the pseudocubic (001)<sub>cub</sub> face, as determined using the Laue XRD technique. Figure 2 shows the morphology of the grown PZNT crystals.

The XRD patterns showed that there was segregation during crystal growth. Segregation was described by an effective segregation coefficient ( $k_{\text{eff}}$ ) using the well-known Burton, Prim, and Slichter equation that relates the growth rate and thickness of the boundary layer:<sup>7</sup>

$$k_{\text{eff}} = \frac{C_S}{C_L} = \frac{k_0}{k_0 + (1 - k_0) \exp\left(-\frac{v}{D} \delta\right)} \quad (1)$$

where  $k_0$  is the equilibrium segregation coefficient (which is a constant for a given solution system),  $D$  the mass diffusion

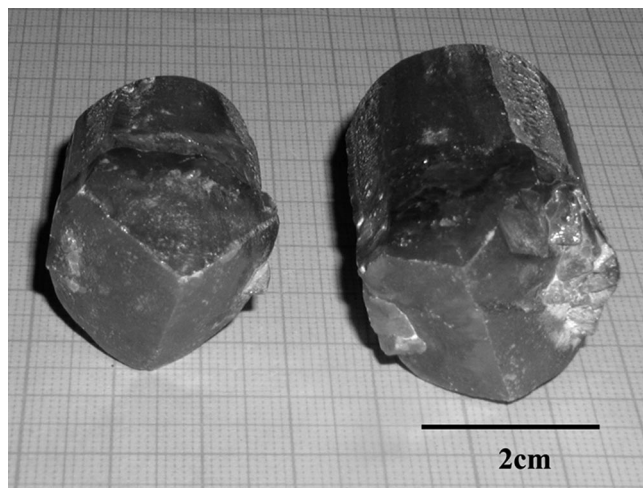


Fig. 2. Morphology of PZNT 91/9 crystals grown by a modified flux Bridgman method.

**Table I. Variation of Composition with Distance from the Seed Crystal in PZNT 91/9 Crystal Grown from an Allomeric PMNT 67/33 Seed Crystal**

Distance, $d$ (mm)	Composition (mol%) <sup>†</sup>					
	PbO	ZnO	Nb <sub>2</sub> O <sub>5</sub>	TiO <sub>2</sub>	Zn <sub>1/3</sub> Nb <sub>2/3</sub>	$x$
2.1–2.6	101.34	28.71	29.35	10.17	87.41	0.1042
8.4–8.9	101.31	28.83	29.43	9.88	87.69	0.1013
16.8–17.3	101.27	28.997	29.43	9.83	87.86	0.1006
23.1–23.6	101.24	28.997	29.44	9.92	87.88	0.1014
Stoichiometry	100.00	30.33	30.33	9.00	91.00	0.09

<sup>†</sup>XRFA results.

coefficient of the solute in a solution system,  $\delta$  the thickness of the boundary layer adjacent to the interface (which relates to the spontaneous convection and the stirring of solution), and  $v$  the growth velocity of the steady-state solid-liquid interface during crystal growth.

This work demonstrates that segregation is not serious during the growth of PZNT single crystals. The composition analysis obtained using XRFA varies with the distance from the seed crystal, as listed in Table I. The accuracy of the XRFA measurement is better than 0.0001 by weight ratio. Within a wafer, there continues to exist variation of composition, which can be revealed using dielectric measurement, but we have not obtained quantitative results.

Because PZNT 91/9 single crystals are grown from PMNT 69/31 seed crystals, the  $PbTiO_3$  content is slightly higher at the

initial stage. From Table I, the segregation coefficient  $k$  for  $PbTiO_3$  content during the crystal growth can be calculated as  $k = C_S/C_L(\infty) = 0.99$ , where  $C_L(\infty)$  is the  $PbTiO_3$  mole concentration at a significant distance from the growth boundary. Therefore, the  $(1-x)PZN-xPT$  system with compositions near the MPB can be considered as almost congruently melting in a narrow range near the seed crystal. At present, high-quality PZNT single crystals with the size of 28 mm in diameter and 30 mm in length of a yellow color have been obtained.

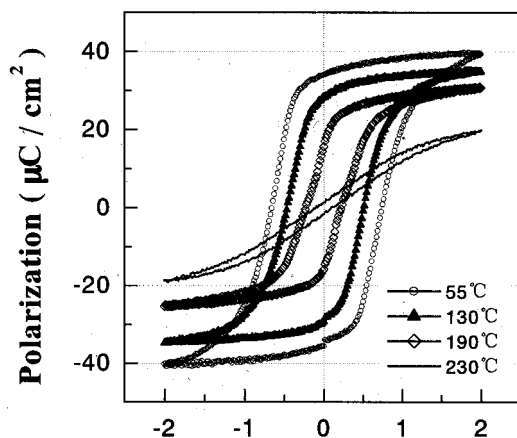
### (3) Ferroelectric Properties

The polarization and strain behavior for the PZNT crystal at various temperatures are shown in Figs. 3(a) and (b). At room temperature, the remnant polarization  $P_r$  of PZNT 91/9 crystal is  $36.5 \mu C/cm^2$ , which is slightly less than the saturation polarization  $P_s$ ,  $40.7 \mu C/cm^2$ , defined as the intercept at zero field of the straight-line portion of the hysteresis loop. The strain of the sample is large. The strain reaches 0.4% at a field of 1.8 kV/mm, which is comparable with that of PZNT crystals grown using the flux method, and it is not yet saturated. Fluctuations of ferroelectric properties within a PZNT (001) crystal wafer are such that  $P_r$  varies between 35.59 and 39.00  $\mu C/cm^2$ , and the coercive field  $E_C$  varies between 5.96 and 7.93 kV/cm. These results denote the heterogeneity of crystal properties caused by the variation of composition and the existence of domain structure.

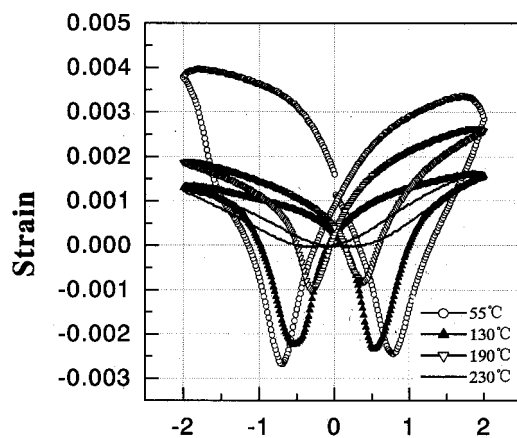
Polarization and strain decrease with an increase of temperature. Polarization and strain decrease sharply between 170° and 190°C, which is consistent with the tetragonal-cubic ferroelectric-paraelectric (FE-PE) phase transition determined using dielectric measurement. When the temperature is higher than the Curie temperature, polarization exists, which indicates FE phase clusters remain to some extent. The temperature dependence of  $P_r$  and  $P_s$  is plotted in Fig. 4. Instead of a gradual polarization dependence on temperature behavior, a sharp change is observed at  $\sim 180^\circ C$ . The thermal behavior implies a metastable character of the crystal near the phase transition.

The temperature dependence of dielectric constant and dielectric loss at various frequencies of an unpoled (001) PZNT 91/9 crystal plate are shown in Fig. 5. There are two apparent anomalies at  $\sim 85^\circ$  and  $183.5^\circ C$  in the dielectric constant curves. This corresponds to the phase transitions from rhombohedral FE phase to tetragonal FE phase and cubic PE phase with increasing temperature. Compared with typical relaxor ferroelectric behavior, the temperature of peak dielectric constant at various frequencies is almost the same. Frequency dispersion continues to exist near the Curie temperature, which indicates that the relaxor behavior exists to some extent.

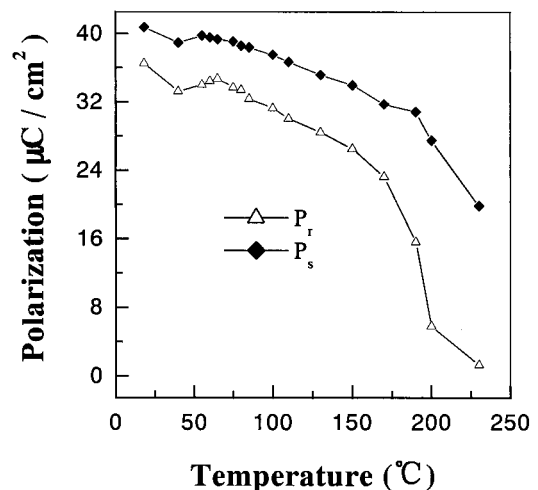
Figure 6 shows the temperature dependence of the real part of the dielectric constant ( $\epsilon'$ ) from heating and cooling processes at the measurement frequency of 1 kHz. Figure 6(b) shows the

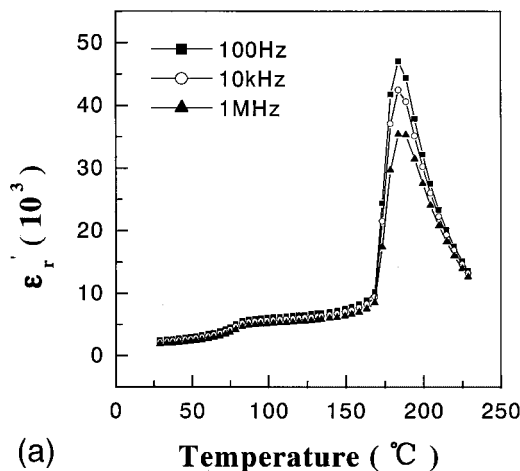


(a) Electric Field (kV / mm)

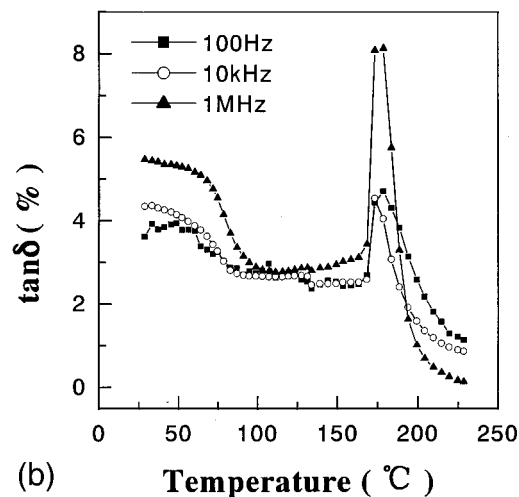


(b) Electric Field (kV / mm)

**Fig. 3.** Hysteresis loops of (a) polarization and (b) strain dependence on the electric field at various temperatures for PZNT 91/9 (001) plane crystal.**Fig. 4.** Temperature dependence of  $P_r$  and  $P_s$  for PZNT 91/9 crystals.



(a) Temperature ( ° C )



(b) Temperature ( ° C )

**Fig. 5.** Temperature dependence of (a) dielectric constant and (b) dielectric loss at various frequencies of an unpoled PZNT 91/9 (001) plane crystal.

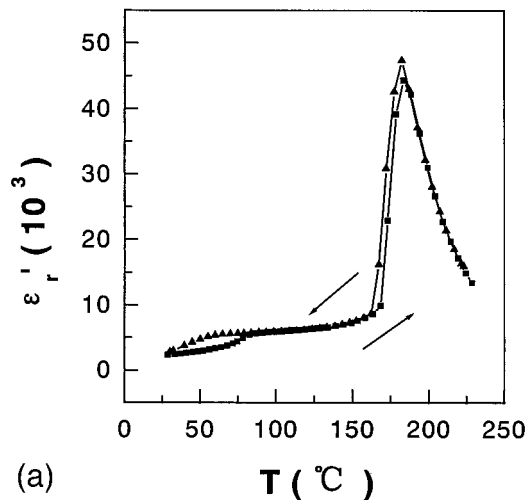
reciprocal behavior of  $\epsilon'$ . Below 80°C, the PZNT 91/9 crystal exhibits a thermal hysteresis across a wide temperature range, whereas, near the Curie temperature, PZNT shows a slight thermal hysteresis.

The electrical properties of the obtained PZNT crystals have been measured. The results indicate that the electrical properties are comparable with those obtained by the vertical Bridgman method PZNT91/9 crystals and the supported Bridgman samples (see Table II).<sup>5,6</sup>

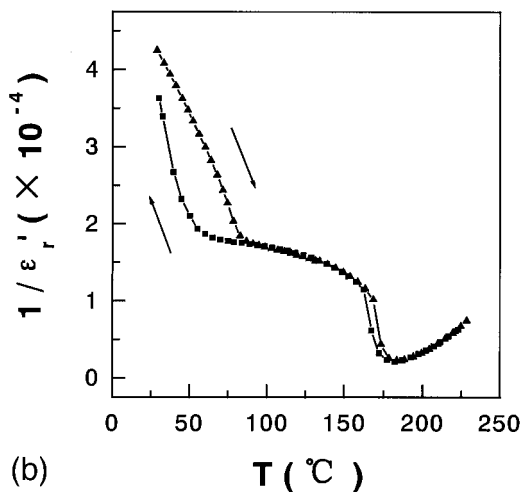
During crystal growth, as the furnace temperature cools through the Curie temperature, the PE–FE phase transition takes place, and ferroelectric domains form. The domain structure is shown in Fig. 7. The striped pattern, characterized by striplike 90° domain walls, which are determined according to the extinction rule, corresponds to the tetragonal phase. Domain observation confirms that the domain structure of the morphotropic PZNT 91/9 crystal has a mixture of rhombohedral and tetragonal orientation states. The optical analysis of the crystal is in agreement with the composition deduced from the dielectric measurement. The rhombohedral phase implies that the  $\text{PbTiO}_3$  concentration is less than the MPB composition. The domain walls for the rhombohedral and tetragonal phase are parallel to  $\{110\}_{\text{cub}}$ . Domain structure and composition fluctuation are regarded as the main causes of the heterogeneity of the electrical properties in PZNT 91/9 single crystals.

#### (4) Characterization of Phase Transition

The physical origins of the temperature-dependent anomalies shown in Figs. 3–6 for the morphotropic PZNT 91/9 single



(a) T ( ° C )



(b) T ( ° C )

**Fig. 6.** (a) Thermal hysteresis behavior of  $\epsilon'_r$  for PZNT 91/9 crystal, taken at 1 kHz and (b) reciprocal of  $\epsilon'_r$ .

crystals are discussed below. The dielectric constant exhibits weak frequency-dependent behavior with a maximum located at  $\sim 183.5^\circ\text{C}$ . This value is consistent with the transition temperature of  $180^\circ\text{C}$  reported by Kuwata *et al.*<sup>2</sup> The low-temperature dielectric anomaly that appears at  $85^\circ\text{C}$  has little dependence on frequency. In addition, a clear thermal hysteresis exists in the temperature regions of  $\sim 155^\circ\text{C} < T < \sim 180^\circ\text{C}$  and  $\sim 30^\circ\text{C} < T < \sim 80^\circ\text{C}$ , which indicates a metastable state near the phase transitions. Polarization and strain continue to exist above the Curie temperature, as shown in Figs. 3 and 4, which indicates ferroelectric clusters exist to some extent. Thus, PZNT 91/9 crystal possesses an almost first-order phase transition with slight diffuse character at  $T_C = 183.5^\circ\text{C}$  from the tetragonal FE phase to the cubic PE phase.

At approximately room temperature, as shown in Fig. 5, the real part of the dielectric constant of the PZNT 91/9 crystal exhibits a weak stepdown with slight frequency dispersion. The dielectric loss also shows a similar tendency. Domain observation confirms that the domain structure of the morphotropic PZNT 91/9 crystal at room temperature has a mixture of rhombohedral and tetragonal phases.<sup>3</sup> Based on the above results, it is concluded that the anomaly of the dielectric constant at  $\sim 85^\circ\text{C}$  in PZNT 91/9 crystal is due to local structural fluctuations between rhombohedral and tetragonal FE clusters. This is a first-order phase transition due to the existence of thermal hysteresis in the dielectric constant. Furthermore, the point groups of the rhombohedral and tetragonal symmetries do not have a group–subgroup relation; therefore, a transition between these phases must be of first order.<sup>11</sup>

**Table II. Summary of Experimental Conditions and Electrical Properties of PZNT 91/9 Crystals Fabricated by Various Bridgman Methods**

Growth method	Vertical Bridgman method (Ref. 5)	Supported Bridgman method (Ref. 6)	Modified Bridgman method (this work)
Dielectric constant (unpoled)	3500–11800	~4000	2500–5000
Dielectric constant (poled)	2100–3700	2500–3500	2000–3000
Dissipation factor, $\tan \delta$ (%)	1.5	2.0	1.3–3.5
Electromechanical coupling factor, $k_t$ (%)	35–57	60	55–64
Rhombohedral–tetragonal phase transition temperature (°C)	48–103		43–84
Curie temperature, $T_C$ (°C)	175–185	170–175	172–186
Maximum temperature of furnace (°C)	1130	1150	1250
Temperature gradient at growing location (°C/cm)	20	17	30–50
Rate of growth (mm/h)	0.2–0.5	0.2–0.5	0.2–0.6

The temperature dependence of the dielectric constant above  $T_m$  fits the empirical formula

$$\frac{1}{\epsilon'_r} = \frac{1}{\epsilon'_{\max}} + \frac{(T - T_m)^\delta}{C'} \quad (2)$$

where  $\epsilon'_{\max}$  corresponds to the maximum value of the dielectric constant at  $T_m$ . The value of  $\delta$  ( $1 \leq \delta \leq 2$ ) is the expression of the degree of dielectric relaxation in a relaxor-based FE material. Based on Eq. (2),  $\delta$  can be determined from the slope of  $\log(\epsilon'_r/\epsilon'_{\max})$  vs  $\log(T - T_m)$ , which is linear in a certain temperature region. When the dielectric data obtained at 1 kHz during heating process are used, a value of  $\delta = 1.27$  is calculated, which indicates that the tetragonal FE–cubic PE phase transition retains the diffuse character to some extent.

#### IV. Conclusions

$Pb((Zn_{1/3}Nb_{2/3})_{0.91}Ti_{0.09})O_3$  (PZNT 91/9) single crystals with a size of 28 mm in diameter and 30 mm in length were successfully grown using a modified Bridgman method with an allomeric seed crystal. Segregation took place during the PZNT crystal growth, which led to composition fluctuation. The segregation also caused the structural phase transition of the PZNT crystals from the rhombohedral phase to the tetragonal phase along the growth

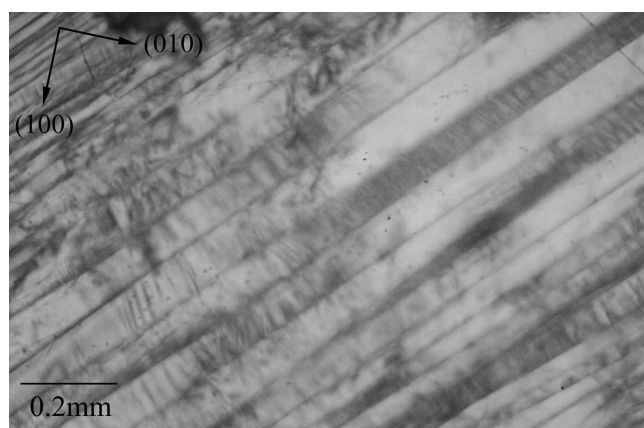


**Fig. 7.** Domain structure in a PZNT mirror-polished (001) plane crystal under crossed polarized light.

direction. Two types of domain structure in the mirror-polished (001)<sub>cub</sub> crystal plate were observed, which indicated that the domain structure of the rhombohedral and tetragonal orientation states coexisted in the PZNT 91/9 crystals. An almost normal FE–PE phase transition was observed at ~183°C. At ~85°C, a weak frequency-dependent FE–FE phase transition was observed that was attributed to a transition between the rhombohedral phase and the tetragonal phase. The thermal hysteresis of the dielectric constant and the existence of polarization above the Curie temperature verified that the phase transitions at ~85° and 183°C were, respectively, first order with a slight diffuse character and first order, respectively. The electric properties of the PZNT crystals varied within the same boule. The fluctuation of composition and the complexity of domain structure were the main reasons for the variation of the boule electric properties. These results demonstrated that the uniformity of the PZNT 91/9 single crystals could be improved by an optimized growth parameter. However, segregation during crystal growth could not be entirely eliminated.

#### References

- 1F. Jiang and S. Kojima, "Raman Scattering of  $0.91Pb(Zn_{1/3}Nb_{2/3})O_3-0.09PbTiO_3$  Relaxor Ferroelectric Single Crystals," *Jpn. J. Appl. Phys.*, **38**, 5128–32 (1999).
- 2J. Kuwata, K. Uchino, and S. Nomura, "Dielectric and Piezoelectric Properties of  $0.91Pb(Zn_{1/3}Nb_{2/3})O_3-0.09PbTiO_3$  Single Crystals," *Jpn. J. Appl. Phys.*, **21** [9] 1298–302 (1982).
- 3Z.-G. Ye, M. Dong, and L. Zhang, "Domain Structures and Phase Transitions of the Relaxor-Based Piezo-Ferroelectric  $(1-x)Pb(Zn_{1/3}Nb_{2/3})O_3-xPbTiO_3$  Single Crystals," *Ferroelectrics*, **229**, 223–32 (1999).
- 4T. Kobayashi, S. Shimanuki, S. Saitoh, and Y. Yamashita, "Improved Growth of Large Lead Zinc Niobate Titanate Piezoelectric Single Crystals for Medical Ultrasonic Transducers," *Jpn. J. Appl. Phys.*, **36**, 6035–38 (1997).
- 5S. Shimanuki, S. Saito, and Y. Yamashita, "Single Crystal of the  $Pb(Zn_{1/3}Nb_{2/3})O_3-PbTiO_3$  System Grown by the Bridgman Method and Its Characterization," *Jpn. J. Appl. Phys.*, **37**, 3382–85 (1998).
- 6K. Harada, Y. Hosono, S. Saitoh, and Y. Yamashita, "Crystal Growth of  $Pb[(Zn_{1/3}Nb_{2/3})_{0.91}Ti_{0.09}]O_3$  Using Crucible by the Supported Bridgman Method," *Jpn. J. Appl. Phys.*, **39**, 3117–20 (2000).
- 7H. Luo, G. Xu, H. Xu, P. Wang, and Z. Yin, "Compositional Homogeneity and Electrical Properties of Lead Magnesium Niobate Titanate Single Crystals Grown by a Modified Bridgman Method," *Jpn. J. Appl. Phys.*, **39**, 5581–85 (2000).
- 8M. Orita, H. Satoh, K. Aizawa, and K. Ametani, "Preparation of Ferroelectric Relaxor  $Pb(Zn_{1/3}Nb_{2/3})O_3-Pb(Mg_{1/3}Nb_{2/3})O_3-PbTiO_3$  by Two-Step Calcination Method," *Jpn. J. Appl. Phys.*, **31**, 3261–64 (1992).
- 9D.-H. Lee and N.-K. Kim, "Crystallographic, Dielectric, and Diffuseness Characteristics of PZN-PT Ceramics," *Mater. Lett.*, **34**, 299–304 (1998).
- 10X. Guisheng, L. Haosu, Z. Weizhuo, Y. Zhiwen, X. Haiqing, and Q. Zhenyi, "Morphology and Defect Structures of Novel Relaxor Ferroelectric Single Crystals  $Pb(Mg_{1/3}Nb_{2/3})O_3-PbTiO_3$ ," *Sci. Sin. (Ser. E)*, **5** [42] 541–49 (1999).
- 11C.-S. Tu, C.-L. Tsai, V. H. Schmidt, H. Luo, and Z. Yin, "Dielectric, Hypersonic, and Domain Anomalies of  $(PbMg_{1/3}Nb_{2/3}O_3)_{1-x}(PbTiO_3)_x$  Single Crystals," *J. Appl. Phys.*, **89** [12] 7908–16 (2001). □